IL NUOVO CIMENTO Vol. 28 C, N. 3 Maggio-Giugno 2005
DOI 10.1393/ncc/i2005-10033-5

The GRB prompt emission from X- to gamma-rays(*)

F. Frontera
University of Ferrara, Department of Physics - Via Paradiso, 12, 44100 Ferrara, Italy
INAF-IASF - via Gobetti, 101, 40129 Bologna, Italy

(ricevuto il 23 Maggio 2005; pubblicato online il 19 Settembre 2005)

Summary. — The status of the Gamma-Ray Burst observations after the *BeppoSAX* switch-off and a summary of the most recent outstanding results obtained from the observational studies of the prompt 2–700 keV emission of GRBs detected with *BeppoSAX* is reported and their impact is discussed.

PACS 98.70.Rz – γ-ray sources, γ-ray bursts.
PACS 01.30.Cc – Conference proceedings.

1. – Introduction

Until the launch of the *BeppoSAX* satellite, all the information about Gamma Ray Bursts (GRBs) was derived from the gamma-ray prompt emission. With the discovery of GRB afterglow emission at longer wavelengths, most of the observational studies were concentrated on the derivations of the properties of this emission and its impact on the physics and origin of the GRB phenomenon. However, it also resulted that, combining together prompt emission and afterglow emission, important key information about GRBs could be derived. *BeppoSAX*, thanks to its configuration with wide (WFCs, 2–28 keV; GRBM, 40–700 keV) and narrow (LECS, 0.1–10 keV; MECS, 2–10 keV; HPGSPC, 4–60 keV; PDS, 15–300 keV) field instruments, was the best satellite for these comparative studies. Indeed all the published BeppoSAX results on single GRBs report the measured properties of the prompt and the afterglow X-ray emission. In addition, a comparative study of these emissions for a sample of GRB was reported [1], and that for the entire sample of *BeppoSAX* GRBs observed with both GRBM and WFCs, is in preparation [2]. From these studies it appears clear that, in synergy with the afterglow observations, the prompt emission continues to play a leading role to understand many open issues, like the GRB emission mechanism, the properties of the GRB environment, the nature of GRB progenitors and the impact of GRBs properties on cosmology.

In this paper, I will review the current observational status of the GRBs detected after the *BeppoSAX* switch-off (30 April 2002) until the launch of the Swift satellite, and some outstanding results derived from the prompt emission study of the *BeppoSAX* GRBs.

(*) Paper presented at the "4th Workshop on Gamma-Ray Burst in the Afterglow Era", Rome, October 18-22, 2004.

2. – GRB observations after the *BeppoSAX* era

Seventy-four GRBs were detected and localized after the BeppoSAX switch-off until October 2004, just before the Swift launch at a mean rate of about 2.5 events/month. Fourty-seven GRBs were detected with HETE2, 18 with INTEGRAL, and 9 with IPN. Sixty-five of them were classical GRBs, and 9 were X-Ray Flashes (XRFs). The redshift was determined for 14 of them and ranged from 0.106 (GRB031203) to 3.37 (GRB030323). All these GRBs, but two (020531, 021201), were long (> 1 s), with their 30–400 keV fluence ranging from 1.6×10^{-8} to 10^{-4} erg cm^{-2}. The most peculiar events were certainly GRB 030329 and GRB031203, both unequivocally associated with Type-Ic supernovae (GRB030329/SN2003dh, [3,4]; GRB031203/SN2003lw, [5]), with GRB031203 being sub-energetic like GRB980425 [6].

The advantage of most of these detections with respect to those obtained with *BeppoSAX* was that their alert was possible in very short times (order of minutes or less). This allowed very prompt optical/near-infrared follow-ups to be performed. However, in spite of these prompt alerts, the X-ray follow-up observations were performed in a small fraction of cases and with notable delays (from 4 hr to 185 hr). Of the 74 GRB detections, only 19 follow-up observations were performed in X-rays: 12 with the *Chandra* (minimum delay of about 15 h), 6 with *XMM-Newton* (minimum delay of about 4 h), and 1 with *Rossi* XTE (delay of 5 h).

3. – Recent observational studies of *BeppoSAX* GRBs

As already reported (see, *e.g.*, [7]), 1082 GRBs were detected with the *BeppoSAX* GRBM, with 51 of which detected also with WFCs and thus accurately localized (see complete list in [8]). Three of the 51 events were X-ray rich (GRB981226, GRB990704, and GRB000615). Of the localized GRBs, 37 were followed-up with the *BeppoSAX* Narrow Field Instruments with a delay ranging from 6 to 21 h. The 40–700 keV fluence of the promptly localized GRBs ranged from 2×10^{-7} to 2×10^{-4} erg cm^{-2}.

This sample, even if relatively small, has allowed to learn most of the basic features of the GRB X-ray afterglows and their relations with the prompt emission. The discovery with *BeppoSAX* of GRB980425 has opened the GRB-supernovae connection issue.

3·1. *Detection of variable column density* $N_{\rm H}$. – In addition to the already reported evidence of variable $N_{\rm H}$ for GRB990705 [9], GRB010214 [10], GRB010222 [11], from the systematic analysis of the WFC plus GRBM data, we have found an outstanding case of decreasing $N_{\rm H}$ in addition to that, already reported, from GRB980329 [1]. The new case of decreasing $N_{\rm H}$ concerns GRB000528 [12].

As fig. 1 shows, in addition to a hard-to-soft spectral evolution, it is apparent a decreasing hydrogen-equivalent column density, which can empirically be described by an exponential function with initial value $N_{\rm H}(t = 0) \sim 2.4 \times 10^{23}$ cm^{-2} (assuming a redshift $z = 0$) and decay constant $t_0 \sim 51$ s.

As in the case of GRB980329, also for GRB000528 the $N_{\rm H}$ continuous decrease is found consistent with a photoionisation process, which is expected when a GRB occurs within a cloud of initially cold gas. In the case of GRB980329 [13], the cloud mass density was found to be $n \sim 4.5 \times 10^5$ cm^{-3} for a composition typical of interstellar matter, and the radial distribution was consistent either with a uniform sphere of radius $R_{sphere} = 0.13$ pc, or a shell at distance $R_{shell} = 0.066$ pc and width $\Delta R = 0.1\, R_{shell}$, with a marginal preference for a shell geometry . Also in the case of GRB980329 [12],

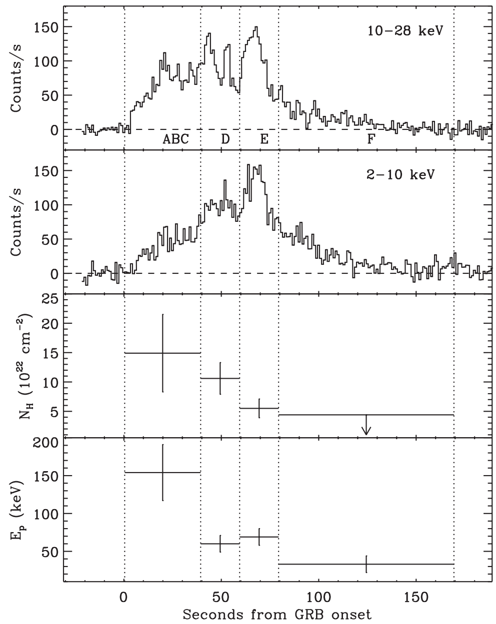

Fig. 1. – Light curve of GRB000528 and the associated time behaviour of the hydrogen equivalent column density and peak energy of the $EF(E)$ spectrum. Reprinted from Frontera et al. [12].

the two cloud geometries (sphere or shell) could not be significantly disentangled, even if it appears, also in this case, a slight preference for the shell geometry. The radius of the cloud has been investigated as a function of the redshift z of the event. In the case of a spherical geometry, it is found to range from 0.029 pc ($z = 0.1$) to 0.162 pc ($z = 0.5$), while in the case of a shell, it ranges from 0.018 pc ($z = 0.1$) to 0.061 pc ($z = 0.5$). Also the initial column density is sensitive to the redshift assumed, ranging from from 6.3×10^{23} cm^{-2} ($z = 0.1$) to 1.0×10^{24} cm^{-2} ($z = 0.5$) in the case of a spherical geometry, and from 3.5×10^{23} cm^{-2} ($z = 0.1$) to 8.9×10^{23} cm^{-2} ($z = 0.5$) in the case of a shell. An initial column density larger than 10^{24} cm^{-2} was not considered since it would affect the γ-ray lightcurve of the GRB. Independently of the redshift and cloud geometry, the best-fit values are all consistent with overdense regions of molecular clouds where star formation takes place, as also found for GRB980329 [13].

A consequent question derived from the these results, is why only in a few cases we find evidence of overdense regions. Indeed, independently of the particular scenario assumed for the origin of the long GRBs (like hypernova model, *e.g.*, [14], or supranova model [15] or quark star transition model [16]), there is general consensus that there is a connection between GRB and supernovae and thus that the pre-burst environment should be characterized by a high-density gas (*e.g.*, [17-19]). The fact that we observe this high-density gas in a few cases, is likely related to the fact the we are observing only the iceberg tip of the N_{H} values associated to GRBs. Only X-ray instruments more sensitive than the SAX/WFCs and/or with lower energy threshold (of the order of 0.1 keV) can show the real density distribution of the circum-burst environment.

3˙2. *New detection of transient absorption features.* – After the discovery of the transient absorption feature in the prompt X-ray spectrum of GRB990705 [9], evi-

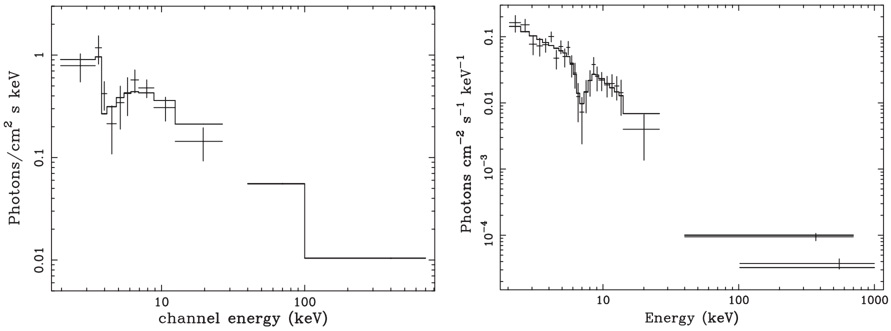

Fig. 2. – Deconvolved spectra of GRB990705 (left) and GRB011211 (right) during the rise time of the events, when a transient absorption feature is visible. Reprinted from Amati *et al.* [9] (left) and Frontera *et al.* [20] (right).

dence of another transient feature is found in the X-ray prompt emission spectrum of GRB011211 [20]. The centroid energy of the feature was 3.8 ± 0.3 keV in the case of GRB990705, it is $6.9^{+0.6}_{-0.5}$ keV in the case of GRB011211. Figure 2 shows the deconvolved spectrum of the GRB990705 and GRB011211 prompt emission in the time interval (the rise of the burst) in which the features are apparent. An asymmetric shape is observed in the case of GRB990705, while in the case of GRB011211 the feature is symmetric.

Both features are found consistent with a resonant scattering of GRB photons off H-like Fe (transition $1s$-$2p$, $E_{rest} = 6.927$ keV) [21]. In this scenario, the line from GRB990705 had to be red-shifted with $z = 0.86 \pm 0.17$ [9], result later found consistent with that of the GRB host galaxy ($z_{opt} = 0.84$, [22]). On the contrary, in the case of GRB011211, the line had to be blue-shifted, implying a highly relativistic outflowing velocity ($v = 0.7c$) of the absorbing material along the line of sight toward the jet cone. In both cases, the circum-burst environment is found typical of a supernova site, *i.e.*, Fe-rich.

Given that any absorption feature in the GRB prompt emission, specially during its rise, implies that the absorbing material is external to the fireball, it appears difficult, if not impossible, to explain these results within the hypernova scenario, given that a delay between supernova explosion and GRB event is required (see discussion in [20]). The supranova model [15] or the quark star transition model [16] appear more suitable.

3$\cdot$3. *Light curve of the early GRB afterglow.* – Since the discovery of the GRB X-ray afterglow with *BeppoSAX*, it resulted a consistency of the flux of the late part of the prompt emission with the back-extrapolation of the power law behaviour of the late afterglow light curve (see, *e.g.*, [23]). An onset time of the X-ray afterglow in corrispondence of the second half of the GRB time duration was later found consistent with the properties of a GRB sample [1].

Recently also the X-ray light curve of the early afterglow has been inferred in three cases: those of GRB011121 and GRB011211 [24], and that of GRB000528 [12]. In all cases, the X-ray afterglow onset appears to be delayed with respect to the GRB onset time, while its early light curve rapidly evolves to a power law behaviour with index consistent with that of the late afterglow. In the case of GRB000528 (see fig. 3), the time origin of the afterglow appears to be at $t = 80$ s from GRB onset. Assuming this time value as time origin, the later prompt emission light curve and late afterglow are

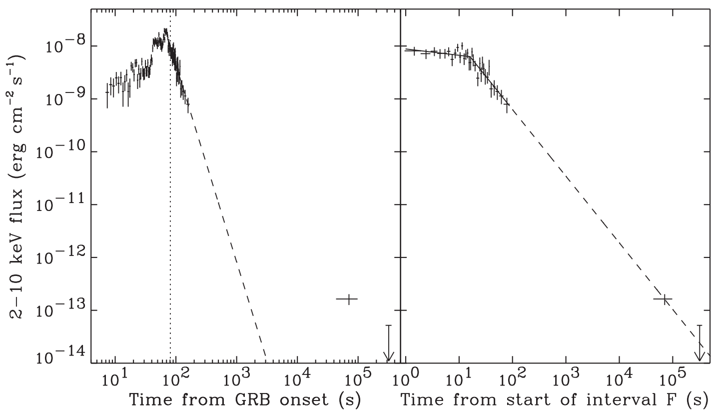

Fig. 3. – 2–10 keV fading curve of GRB000528. The afterglow upper limit is at 2σ level. The vertical dotted line in the left panel shows the likely beginning of the afterglow. *Left panel:* light curve of the GRB and its late afterglow assuming as origin the onset time of the GRB. The best fit of the late light curve ($t > 80$ s) and its extrapolation at later times is also shown. It can be seen it does not fit the late afterglow data points. *Right panel:* The late GRB light curve and its extrapolation at later epochs, when the time $t = 80$ s is assumed as origin of the afterglow onset time. Reprinted from Frontera *et al.* [12]

well fit with a broken power law, with index $\delta_1 \sim 0.12$ for $t < t_b \sim 16$ s, while for $t > t_b$, $\delta_2 \sim 1.3$. Decay law and spectrum of the early afterglow ($t > 80$ s) for this GRB are consistent with the expectations of the external shock model, during the fast cooling phase and the thick shell regime [25].

3·4. *E_p vs. L_{iso} relation within single GRBs.* – The E_p-*vs.*-E_{iso} relationship for GRBs is well known [26]. It establishes a relation ($E_p \propto E_{iso}^{\alpha}$ with $\alpha \sim 0.5$) between the peak energy E_p of the $\nu F(\nu)$ spectrum in the cosmological rest frame and the isotropic-equivalent energy radiated in the GRBs events. A similar relation is found if E_{iso} is replaced by the GRB peak luminosity L_{iso}^{p} [27]. Both E_p and E_{iso} (or L_{iso}^{p}) are evaluated from the time-averaged spectra of GRBs with known z. Recently Ghirlanda *et al.* [28], following Frail *et al.* [29] and Bloom *et al.* [30], for a sample of 24 GRBs with known redshift and known jet break time, derived the collimation-corrected radiated energy E_γ, and found a tight correlation between E_p and E_γ ($E_p \propto E_\gamma^{\alpha}$ with $\alpha \sim 0.7$), in the assumption of a constant energy conversion efficiency $\eta = 0.2$ and using, for each GRB in the sample, the best density estimates of the curcumburst medium. Unlike the results by Amati *et al.* [26], those derived by Ghirlanda *et al.* [28] are model dependent.

In order to clarify the physics under these relations, we are performing a systematic study of the spectral evolution of all GRBs detected with the *BeppoSAX* GRBM and WFCs. We have derived, in each of the time intervals in which each GRB light curve was subdivided (number depending on the GRB brightness), the measured peak energy E_p^m and the corresponding 2–700 keV flux F. For the GRBs with known redshift, we have also derived the intrinsic E_p and the corresponding luminosity. The results are the subject of a paper in preparation (Frontera *et al.* [2]). Figure 4 shows an example of result obtained for GRB970111, a GRB with unknown z. We find that in general a power law fits the data, for either GRB with known or unknown z. For those with known z, merging all together the (E_p, L_{iso}) data points, we find that they well correlate

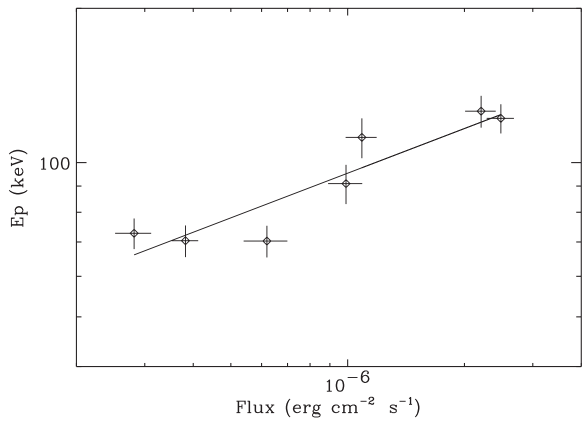

Fig. 4. – The measured peak energy E_p *vs.* 2–700 keV flux in the 7 time intervals in which the light curve of GRB 970111 is subdivided.

($\chi_r^2 = 0.86$) with each other according to a power law with $\alpha \sim 0.5$. The correlation is also found between E_p and L_γ with $\alpha \sim 0.65$, that is almost similar to that (~ 0.7) reported by Ghirlanda *et al.* [28], but with a seemingly higher spread ($\chi_r^2 = 1.69$) than that found for the E_p-*vs.*-L_{iso} correlation. Consequences of these results will be discussed in the paper by Frontera *et al.* [2].

3·5. *Evidence of a long duration gamma-ray component in short* ($<$ 1s) GRBs. – The prompt and accurate localization of short GRBs is crucial to discover their counterparts, if any, at lower wavelengths. No short GRB was promptly detected with the SAX/WFCs in spite of the 168 short events detected with GRBM [7]. Two short GRBs (020113, and 020531) were localized with HETE2, but no identification at lower wavelengths was obtained, in spite that GRB020531 was promptly followed up in the optical band since 90 min after the primary event [31]. *Chandra*, 5 days after the main event, obtained an X-ray upper limit of 2×10^{-15} erg cm^{-2}s^{-1} [32]. From these observations it appears that, if present, the afterglow from GRB020531 should be either much weaker than the weakest afterglow observed from long GRBs, or it should be of very short duration and/or with a very fast fading. The search for afterglow emission from short GRBs is of key importance to establish the origin of these still mysterious events.

Search of afterglow emission in gamma-rays has already been performed by summing together many aligned background light curves around short events. Connaughton [33] found a marginal post-burst excess of 100 s duration by summing together 100 aligned BATSE light curves ($>$ 20 keV). Lazzati *et al.* [34], summing together 76 BATSE light curves, found a weak post-burst excess in the 25–100 keV energy band, that peaked about 30 s after the burst time and was visible for about 100 s. The excess peak flux at 50 keV is $\sim 10^{-11}$ erg cm^{-2}s^{-1}keV^{-1}, while its integrated energy spectrum ($F(\nu) \propto \nu^{-1.5}$) is softer than that of any detected short GRBs. The excess was interpreted by Lazzati *et al.* as afterglow emission.

Following the Lazzati *et al.* [34] method, we have selected 93 short GRBs detected with the *BeppoSAX* GRBM, finding the presence of an excess that, unlike the Lazzati result, starts $\sim$ 20 s before the burst and ends $\sim$ 30 s after the event [35]. Figure 5 shows the time behaviour of the 40–700 keV cumulative excess. The signal is found higher in

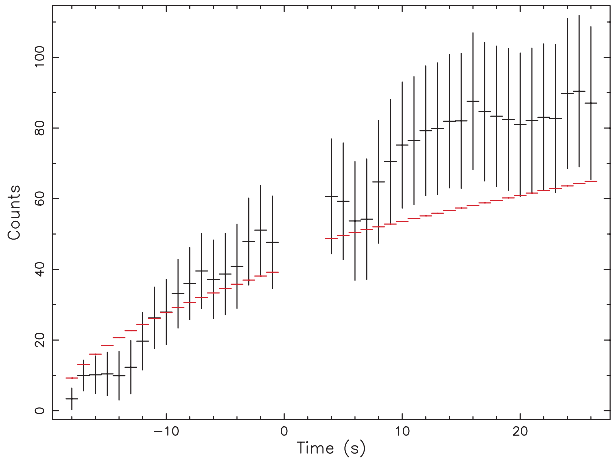

Fig. 5. – Cumulative 40–700 keV counts per burst of the average background-subtracted light curves *vs.* time from -19 s assumed as origin of the time axis. Dashed marks gives the $3\,\sigma$ level of the cumulative excess. Reprinted from Montanari *et al.* [35]

the 40–700 keV band than above 100 keV. The spectral hardness of the excess is slightly lower than that of the main event before the burst, and becomes similar later. Its time averaged 40–700 keV flux is $\sim 3\times10^{-9}\,\mathrm{erg\,cm^{-2}\,s^{-1}}$, which is only a few percent of that of the GRB ($5.5\times10^{-7}\,\mathrm{erg\,cm^{-2}\,s^{-1}}$), while the 40–700 keV fluence ($1.3\times10^{-7}\,\mathrm{erg\,cm^{-2}}$) is comparable to that of the main events. Our results point to a prompt emission component rather than an early afterglow as origin of the found excess. Understanding the origin of this component can greatly help to understand the nature of short GRBs.

4. – Conclusions

The *BeppoSAX* data archive on the GRB prompt emission is still continuing to provide outstanding results. Among those recently obtained, I have discussed some of the most relevant. We have discovered a rapidly decreasing hydrogen-equivalent column density N_{H} of the circumburst medium along the line of sight of GRB000528. We have found a new evidence of a transient absorption feature during the rise of GRB011211. We have inferred the early afterglow light curve of GRB000528. From the study of the time-resolved spectra, we have found a tight correlation between measured peak energy E_p^m of the $EF(E)$ spectrum and corresponding flux $F(t)$ within single GRBs of known or unknown redshift. For GRBs with known z, this correlation reflects in a similar correlation between $E_p(t)$ and $L_{iso}(t)$ and between $E_p(t)$ and the collimation corrected luminosity $L_\gamma(t)$. In addition, superposing all the time-resolved (E_p, L_{iso}) or (E_p, L_γ) data points, we confirm both the Amati [26] and Ghirlanda [28] relations, finding a tighter correlation between $E_p(t)$ and $L_{iso}(t)$ rather than between $E_p(t)$ and $L_\gamma(t)$. Finally we find evidence of a weak and long duration component from short GRBs, that starts before the main events. The study of the origin of this emission can bring to the understanding of the nature of short GRBs.

The SWIFT mission is expected to settle many open issues left open by *BeppoSAX* but not all. The confirmation of the reported transient absorption features, the study of the GRB N_{H}, the light curve of GRBs from the GRB onset to the late afterglow in the same energy band, will require other missions, like *Lobster–ISS* [36, 37].

* * *

I wish to thank E. Maiorano for helping me to collect the information reported in this paper on GRBs detected in the post *BeppoSAX* era. This work was supported by the Ministry of Education, University and Research of Italy (PRIN 2003-020775).

REFERENCES

[1] Frontera F. *et al.* , *ApJS*, **127** (2000) 59.
[2] Frontera F. *et al.* , to be submitted to *ApJ*.
[3] Stanek K. Z. *et al.* , *ApJ*, **591** (2003) L17.
[4] Hjorth J. *et al.* , *Nature*, **423** (2003) 847.
[5] Malesani D. *et al.* , *ApJ*, **609** (2004) L5.
[6] Soderberg A. M. *et al.* , *Nature*, **430** (2004) 648.
[7] Frontera F., in *Gamma-Ray Bursts: 30 Years of Discovery*, edited by E. E. Fenimore and M. Galassi, *AIP Conf. Proc.*, **727** (2004) 31–36.
[8] Frontera F., in *Gamma-Ray Bursts in the Afterglow Era*, edited by M. Feroci, F. Frontera, N. Masetti and L. Piro, *ASP Conf. Proc.*, **312** (2004) 3-11.
[9] Amati L. *et al.* , *Science*, **290** (2000) 953.
[10] Guidorzi C. *et al.* , *A&A*, **401** (2003) 491.
[11] in't Zand J.J.M. *et al.* , *ApJ*, **559** (2001) 710.
[12] Frontera F. *et al.* , *ApJ*, **614** (2004) 301.
[13] Lazzati D. & Perna R., *MNRAS*, **330** (2002) 383.
[14] Paczynski B., *ApJ*, **494** (1998) L45.
[15] Vietri M. & Stella L., *ApJ*, **507** (1998) L45.
[16] Berezhiani Z. *et al.* , *ApJ*, **586** (2003) 1850.
[17] Lazzati D. *et al.* , *MNRAS*, **304** (1999) L31.
[18] Böttcher M., *ApJ*, **539** (2000) 102.
[19] Weth C. *et al.* , *ApJ*, **534** (2000) 581.
[20] Frontera F. *et al.* , *ApJ*, **616** (2004) 1078.
[21] Lazzati D. *et al.* , *ApJ*, **556** (2001) 471.
[22] Le Floc'h E. *et al.* , *ApJ*, **581** (2002) L81.
[23] Costa E. *et al.* , *Nature*, **387** (1997) 783.
[24] Piro L. *et al.* , *ApJ*, **623** (2005) 314.
[25] Sari R. & Piran T., *ApJ*, **520** (1999) 641.
[26] Amati L. *et al.* , *A&A*, **390** (2002) 81.
[27] Yonetoku D. *et al.* , *ApJ*, **609** (2004) 935.
[28] Ghirlanda G. *et al.* , *ApJ*, **616** (2004) 331.
[29] Frail D. A. *et al.* , *ApJ*, **562** (2001) L55.
[30] Bloom J. S. *et al.* , *ApJ*, **594** (2003) 674.
[31] Klotz A., Boer M. and Atteia J. L., *A&A*, **404** (2003) 815.
[32] Butler N. *et al.* , in *Third Rome Workshop on Gamma-Ray Bursts in the Afterglow Era*, edited by M. Feroci, F. Frontera, N. Masetti, and L. Piro, *ASP Conf. Proc.*, **312** (2004) 201.
[33] Connaughton V., *ApJ*, **567** (2002) 1028.
[34] Lazzati *et al.* , *A&A*, **379** (2001) L39.
[35] Montanari E. *et al.* , *ApJ*, **625** (2005) L17.
[36] Amati *et al.* 2005, to be published in *Adv. Space Res.*
[37] Frontera F. *et al.* , in these Proceedings.